

Elsevier Editorial System(tm) for Planetary and Space Science  
Manuscript Draft

Manuscript Number:

Title: THE C1XS X-RAY SPECTROMETER ON CHANDRAYAAN-1.

Article Type: Research Paper

Keywords: Moon  
Lunar Composition  
X ray spectroscopy  
Chandrayaan-1  
Space Instrumentation

Corresponding Author: Prof. Manuel Grande,

Corresponding Author's Institution: Aberystwyth University

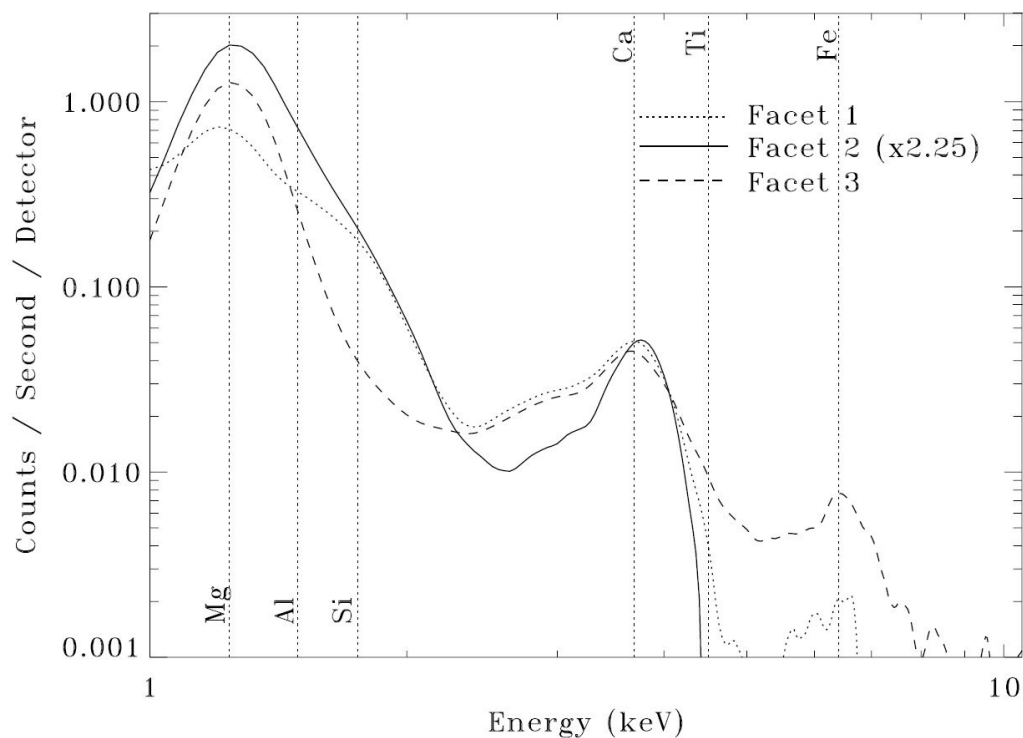
First Author: Manuel Grande

Order of Authors: Manuel Grande; Brian Maddison; chris J Howe; Barry J Kellett; P Shreekumar; Juhani Huovelin; Ian Crawford; Lionel C d'Uston; David Smith; Manesh Anand; Narendra Bhandari; Antony T Cook; Vera Fernandes; Bernard Foing; Olivier Gasnault; J N Goswami; Andrew Hollang; Katie H Joy; Detlev Kochney; David Lawrence; Sylvestre Maurice; T Okada; Syama Narendrath; Carle Pieters; David Rothery; Sara S Russell; Alok Shrivastava; Bruce Swinyard; Martin Wilding; Mark Wieczorek

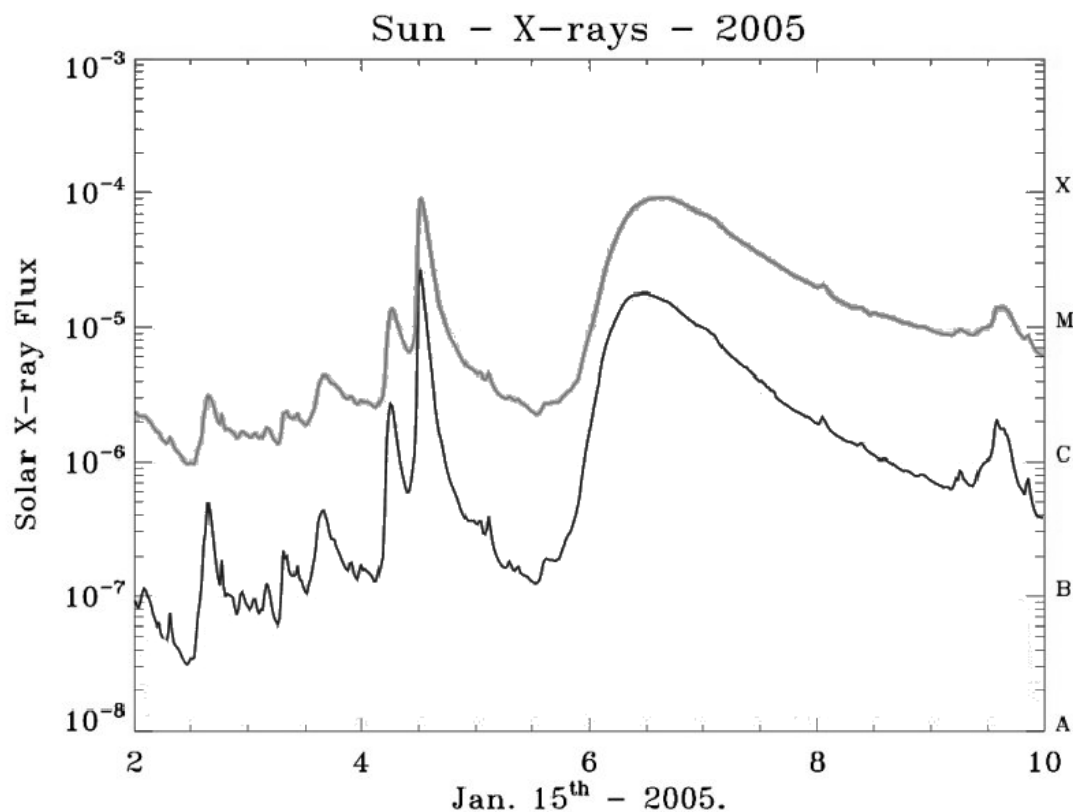
Abstract: The Chandrayaan-1 X-ray Spectrometer (C1XS) is a compact X-ray spectrometer for the Indian Space Research Organisation (ISRO) Chandrayaan-1 lunar mission. It exploits heritage from the D-CIXS instrument on ESA's SMART-1 mission. As a result of detailed developments to all aspects of the design, its performance as measured in the laboratory greatly surpasses that of D-CIXS. In comparison with SMART-1, Chandrayaan-1 is a science oriented rather than a technology mission, leading to far more favourable conditions for science measurements. C1XS is

designed to measure absolute and relative abundances of major rock-forming elements (principally Mg, Al, Si, Ca and Fe) in the lunar crust with spatial resolution  $\leq 25$  FWHM km, and to achieve relative elemental abundances of better than 10%.

Figure 1



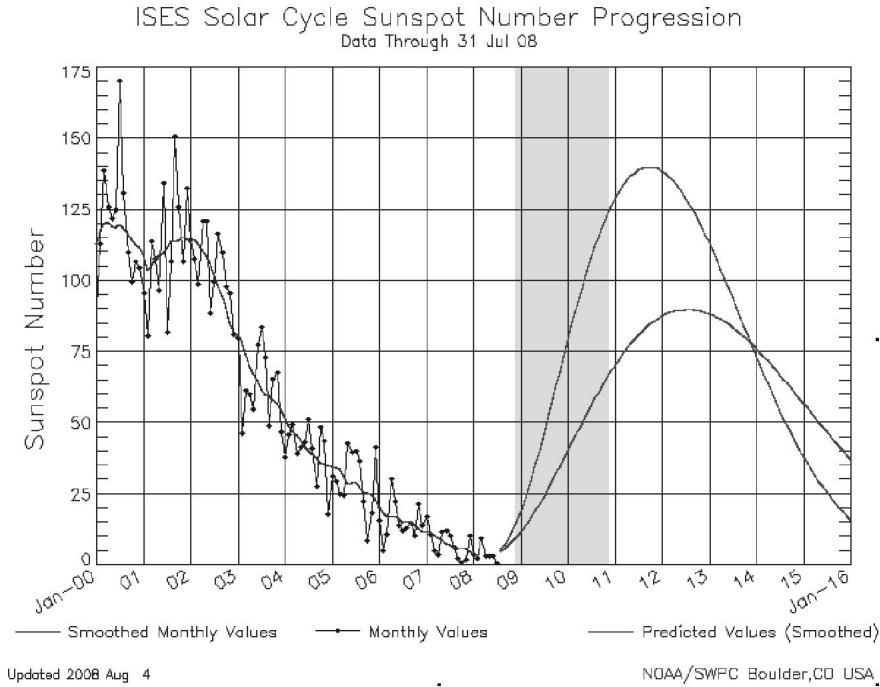
a)



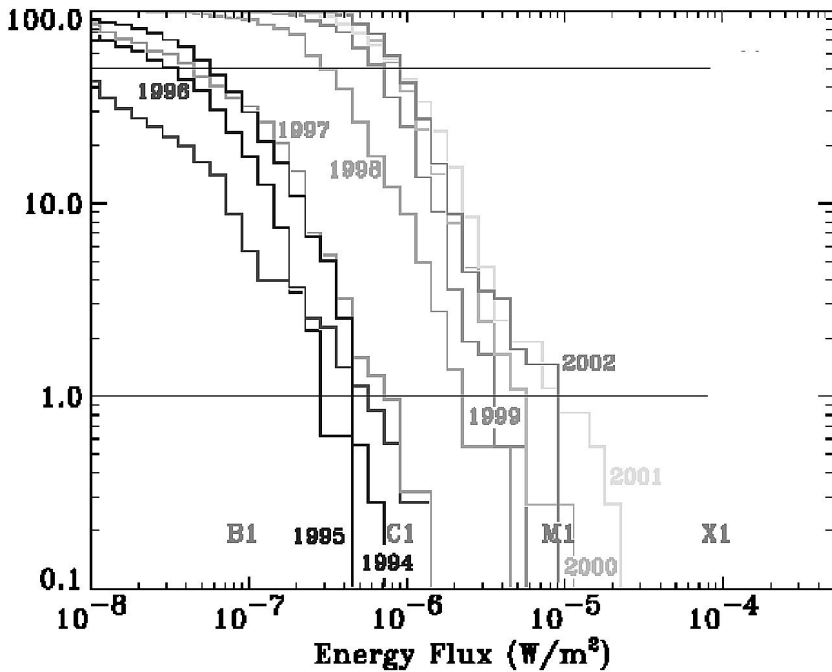
b)

**Figure 1:** a) Fluorescence spectra obtained by D-CIXS on SMART-1 on 15 Jan 2005, indicating an ability to remote sense elements in the top few micrometers of the Lunar regolith, in particular Mg, Al, Si, Ca and Fe, as indicated by vertical lines (Grande et al 2007). Vertical lines indicate the expected position of these elements. b) Also shown is the 10Å (black) and 1 Å (grey) (TBC) Solar X-ray illumination at the time, derived from GOES data, indicating the high variability of the Sun as an X-ray source. Times are indicated on the X axis in hours. Note the conventional A,B,C,M,X nomenclature for flare levels are indicated on the left hand side of the plot.

Figure 2



a)

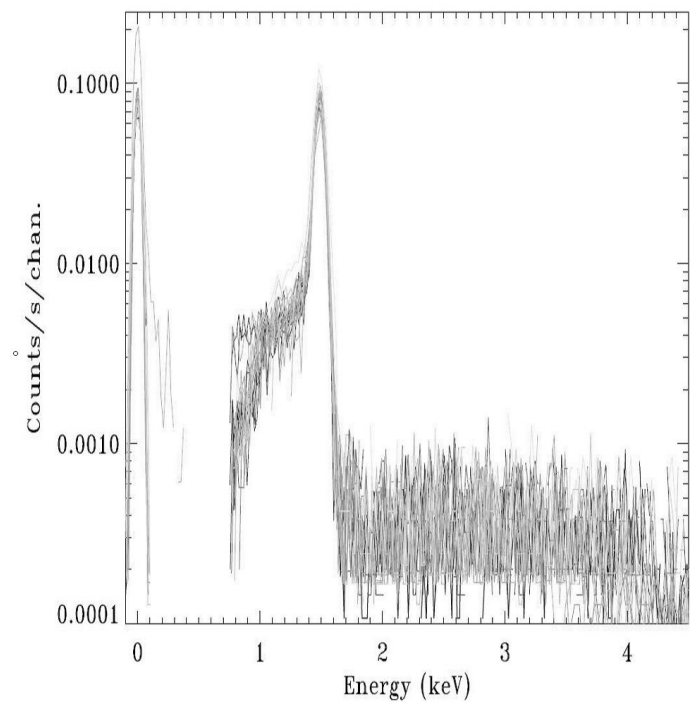


b)

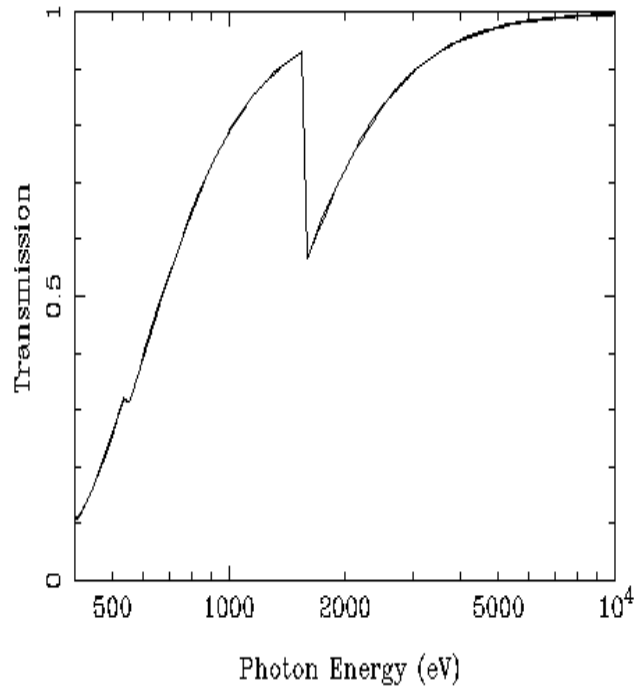
**Figure 2 (a)** Past blue and predicted red solar cycle variation (NOAA Space Weather Prediction Center) during the Chandrayaan-1 missions (Ref). Note that whilst SMART-1 took place during a decline into solar minimum, Chandrayaan-1 will be launched in the ascending phase of the cycle (shown by shaded region), which is predicted to be close to peak by the end of the mission. The two red lines indicate alternative predictions.

(b) cumulative distribution of one minute solar flare data from the previous cycle, indicating probability of illumination above a certain illumination level more. To obtain predicted fluxes add 11 to the year.

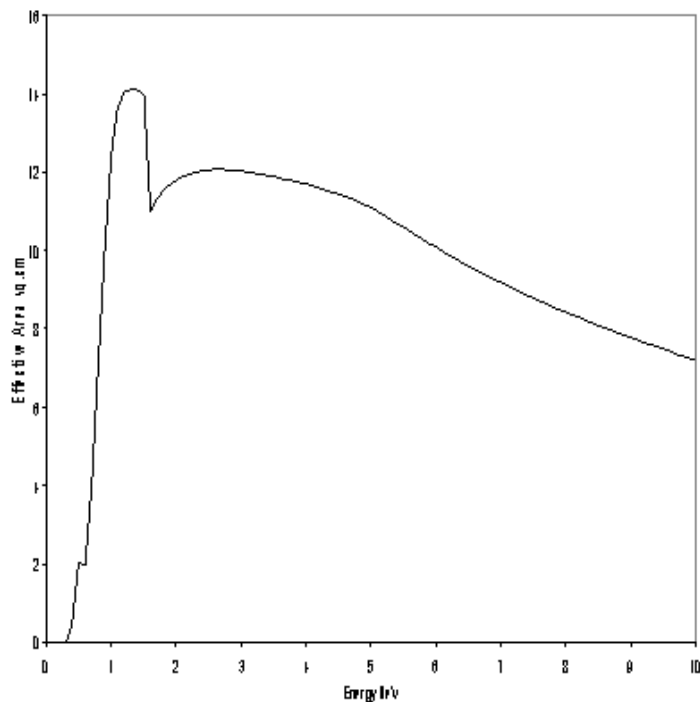
Figure 3



a)



b)



c)

**Figure 3:** (a) Measured performance at low energies in CIXS illustrating the response of all 24 SCDs to Al K $\alpha$  (1.487 keV) and the low energy cut off of the instrument at 750 eV, derived during calibration (Kellett et al forthcoming). Note the excellent alignment and uniformity of the 24 different responses. (b) calculated filter transmission for 800 nm of Al coated Polyimide over the active range of the instrument. (c) Calculated effective area of the instrument, plotted against energy, based on geometry, and filter and detector specification, but neglecting electronic losses. Note the rapid loss of effective area below 1 keV.

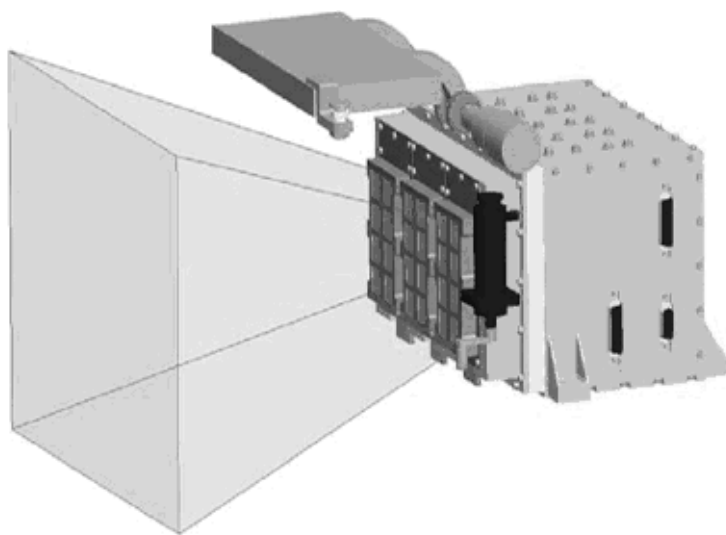


**Figure 4:** CAD image of the C1XS instrument showing coalligned front detectors, deployable radiation shield and  $14^{\circ}$  Field of View. Note light coloured thermal gasket separating cool detector enclosure from electronics case to the right.

The instrument design aims to keep detector temperatures below  $-17.5\text{ C}$ , which ensures optimum signal to noise and stability, as well as improving radiation tolerance.

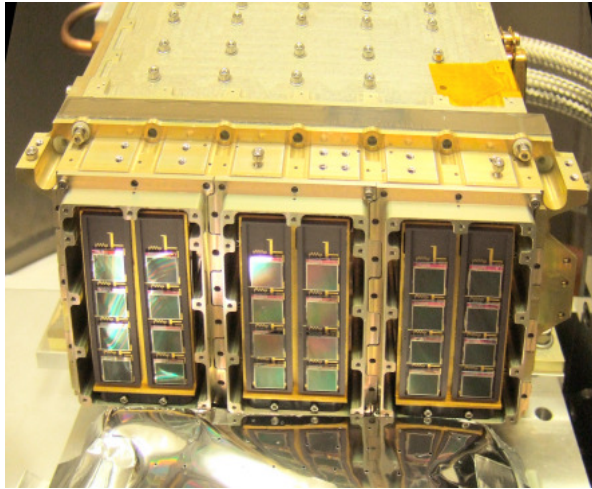
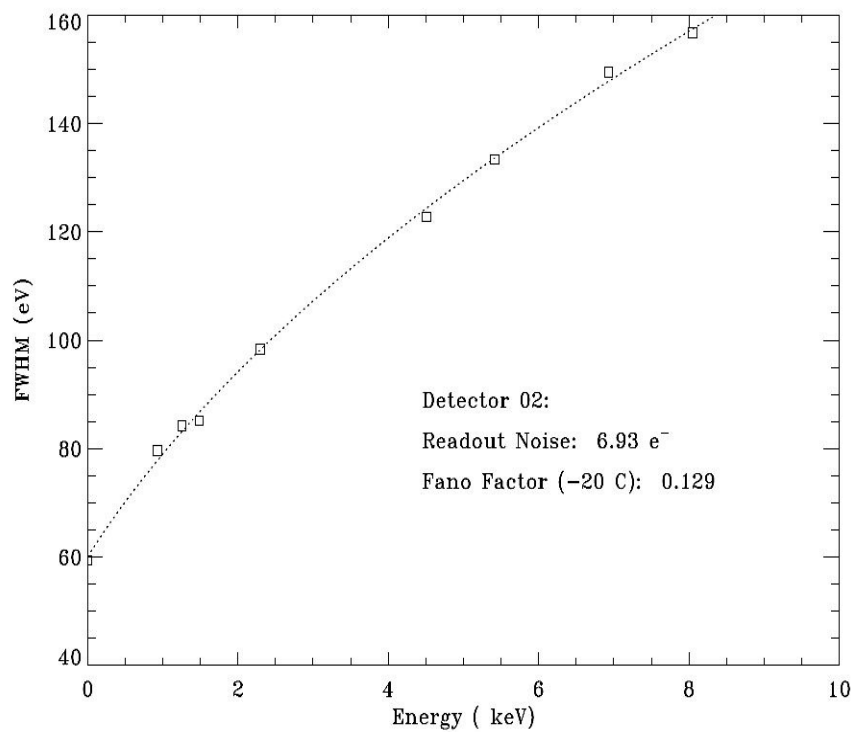
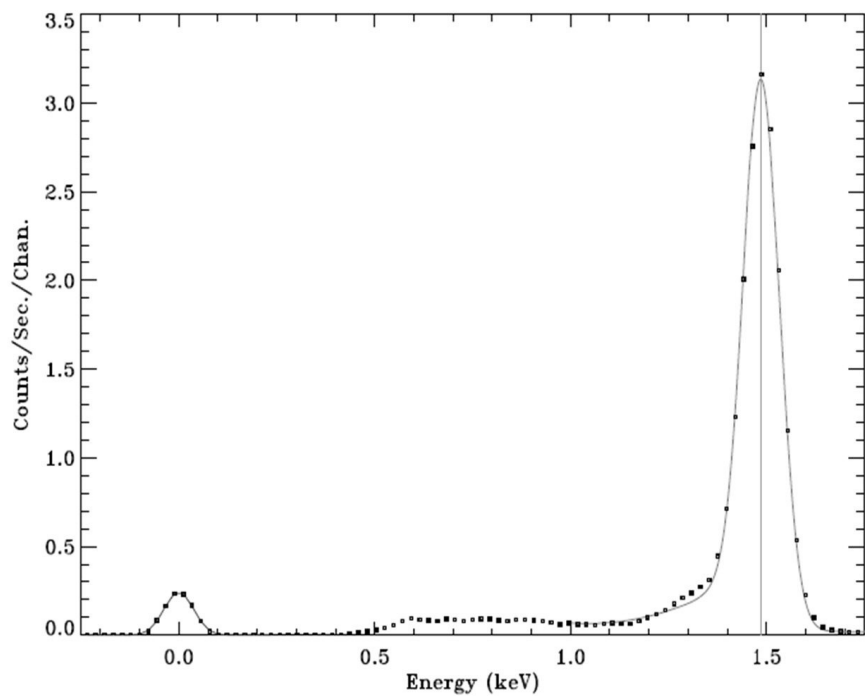


**Figure 5:** View of the C1XS flight instrument during calibration. The collimator assembly and doors have not yet been added, so that the 24 swept charge detectors, arranged in ladders of four, are clearly seen.

Figure 6



a)



b)

**Figure 6:** Laboratory performance of C1XS as obtained during calibration (Kellett et al 2008). (a) Measured combined FWHM of the detectors and readout electronics as a function of energy. (b) Example showing measured resolution at the 1.49 keV Aluminium  $K\alpha_1$  line and also the well separated zero energy electronic noise peak. Note the major improvement over the performance of D-CIXS shown in Figure 1.



Figure 7

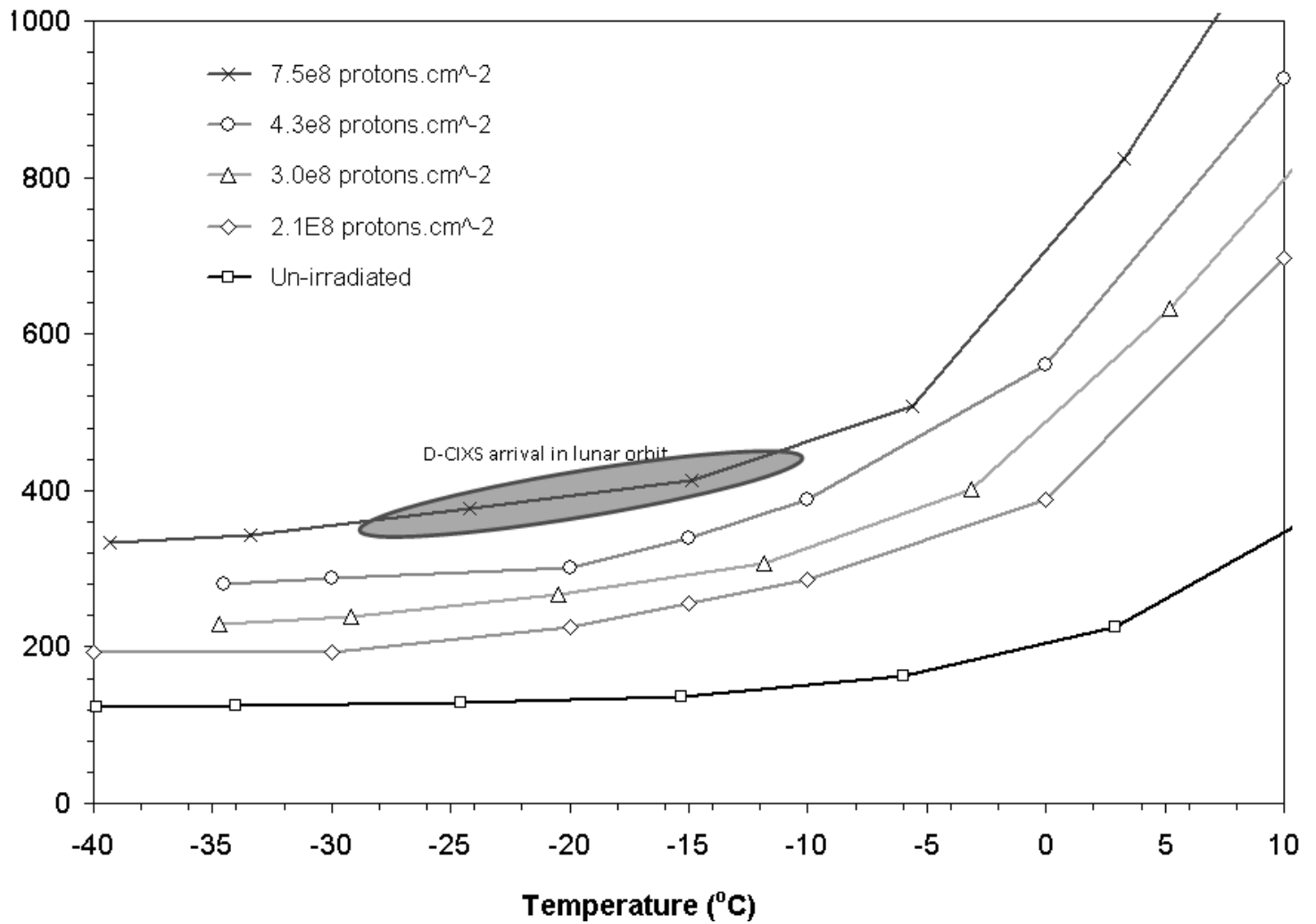
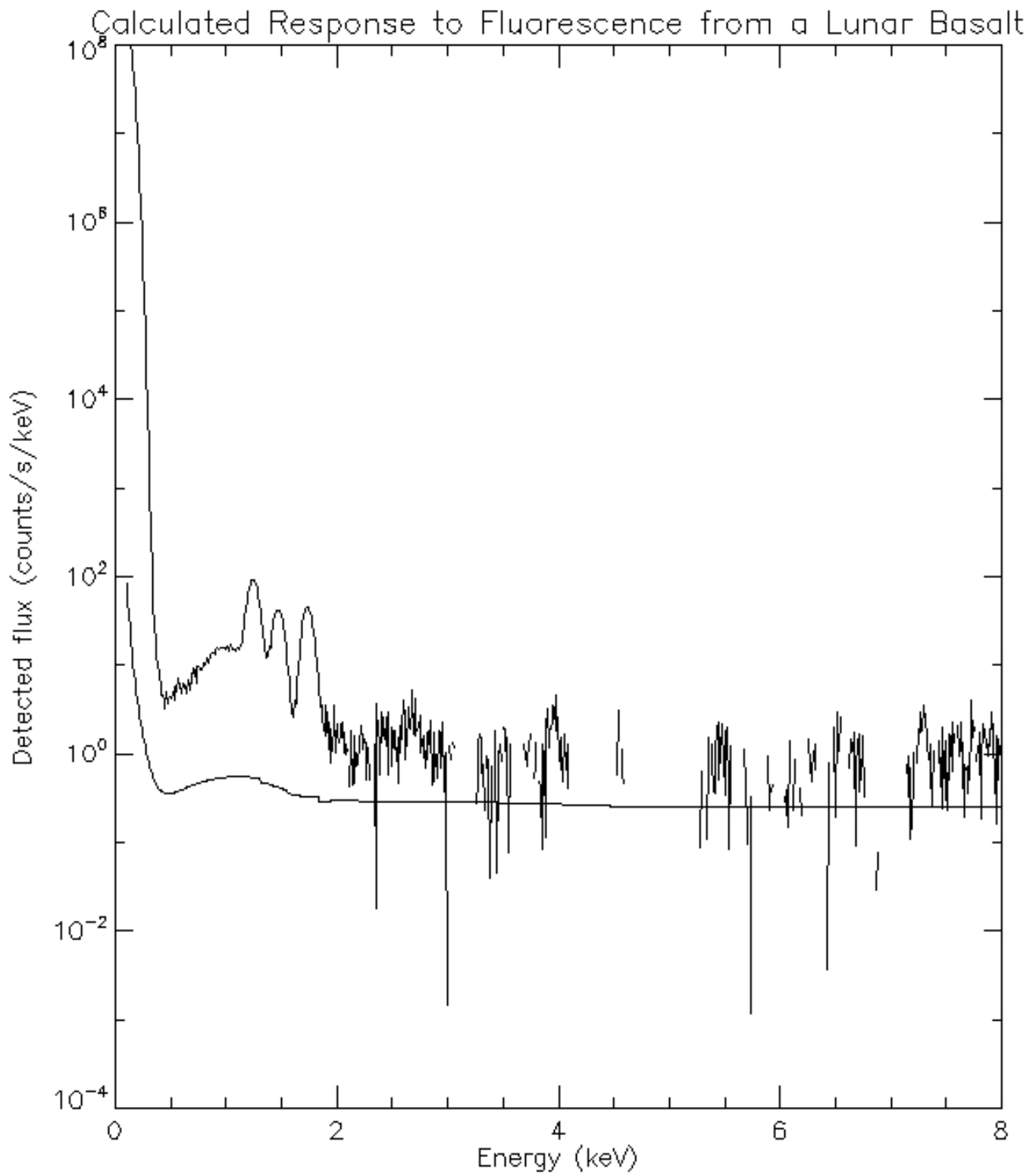


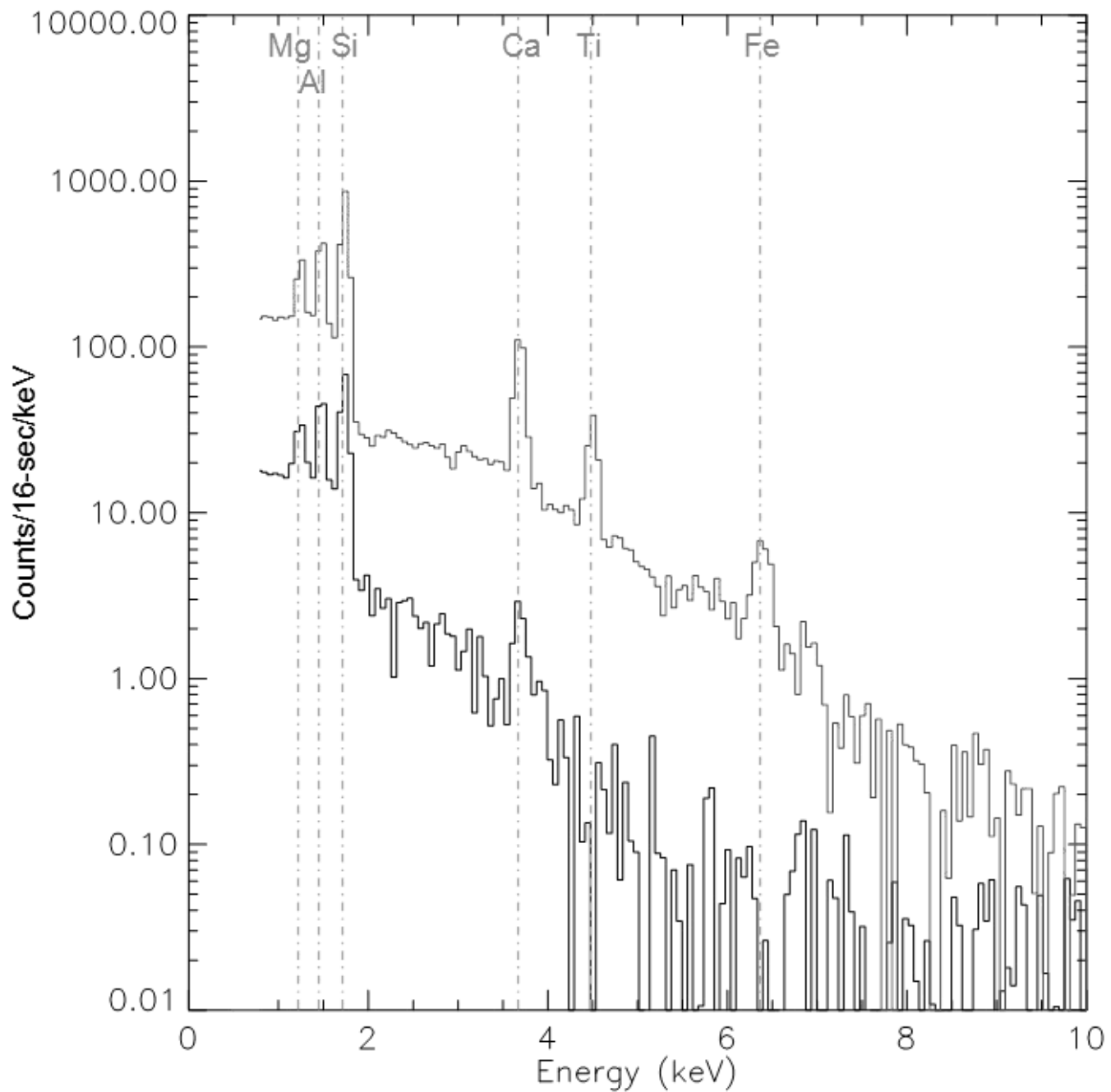
Figure 7: Swept charge device energy resolution shown as FWHM at the Mn-K $\alpha$  line vs. temperature, before and after radiation testing. The specified maximum operating temperature is -17.5°C. Note the favourable comparison with D-CIXS FWHM shown in between the dashed lines.

Figure 8



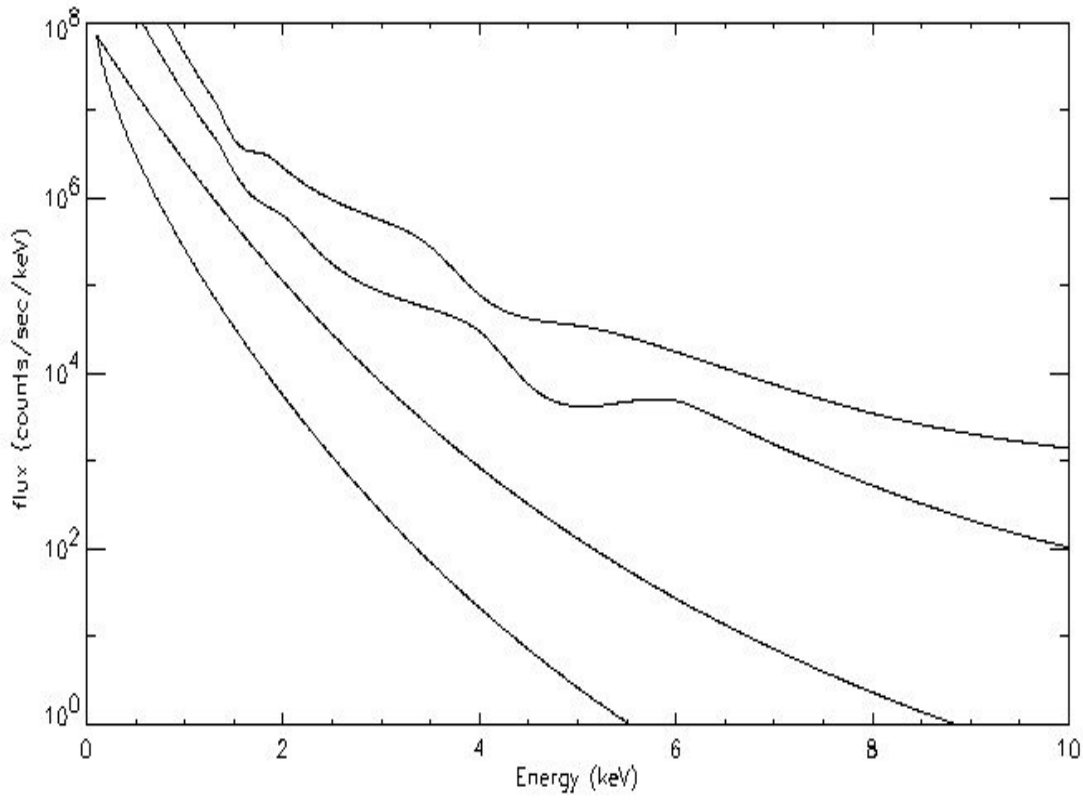
**Figure 8** Calculated response to fluorescence from a representative Lunar basalt, using our physical instrument model, indicating the minimum detectable flux for C1 flare with a 14 deg opening angle for a real detector area of 24 cm<sup>2</sup> detector and a 0.8 throughput collimator expressed as counts/sec/keV and 100 eV resolution. The calculation includes calibration and electronic efficiency data from D-CIXS. The smooth line is the 3 sigma detection limit for a 16 second integration, typical for overflight of a single pixel. It is seen that the Mg, Al and Si lines are well resolved in this baseline illumination condition.

Figure 9

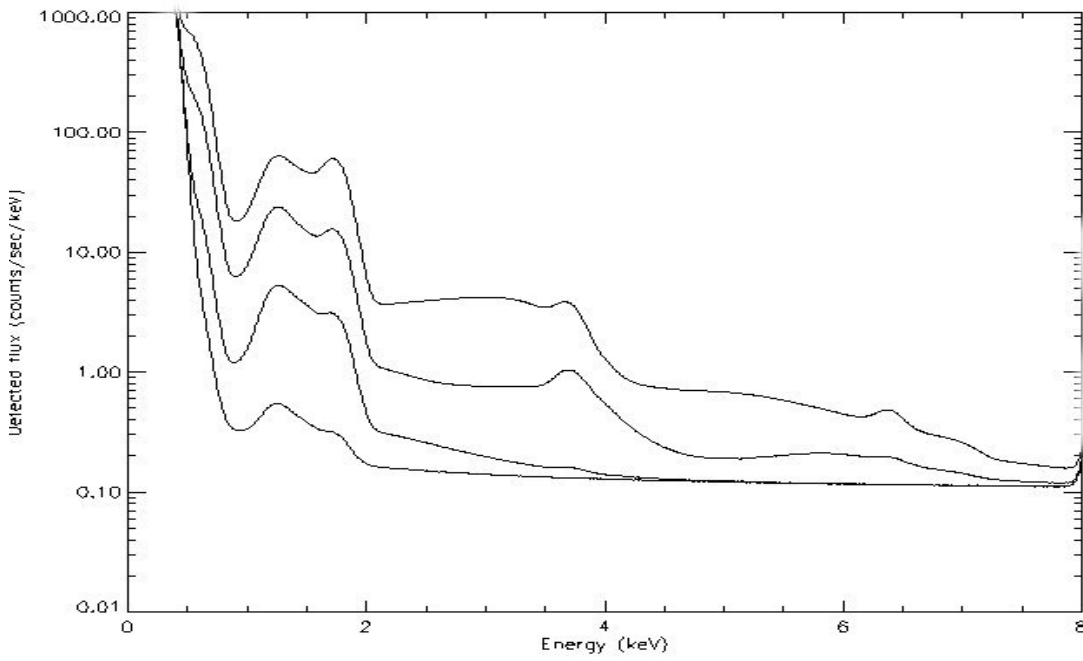


**Figure 9.** Simulated C1XS spectrum for the November 18 flare based on individual 16 second integrations. The lower line (black) shows the spectrum detected during the quiet period just before flare begins, while the upper line (grey) shows the spectrum obtained at the peak of the flare.

Figure 10



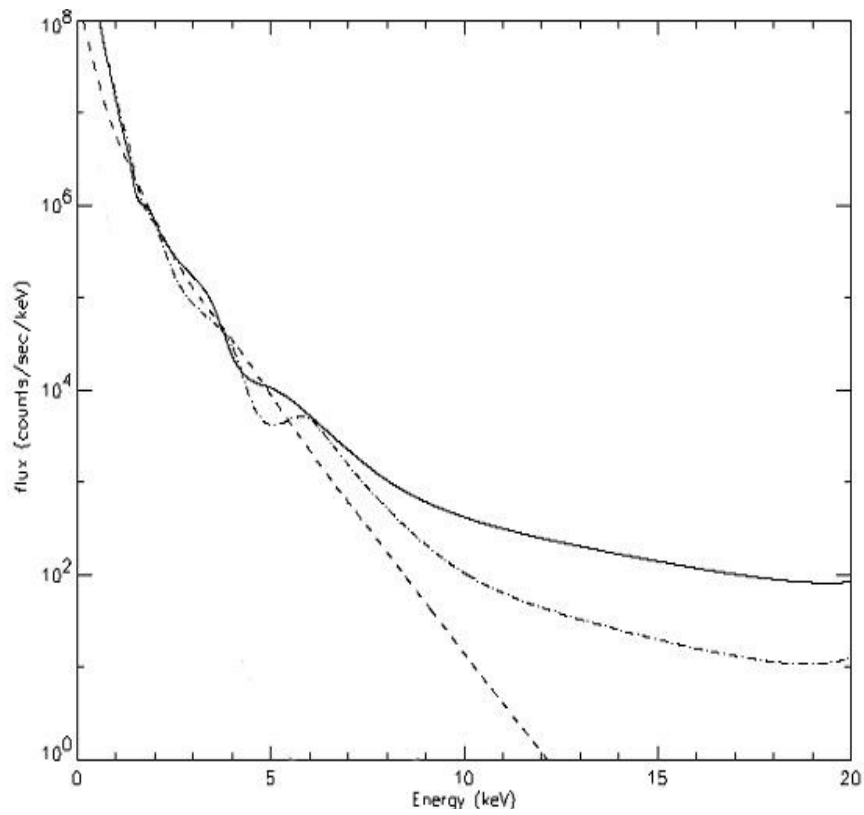
a)



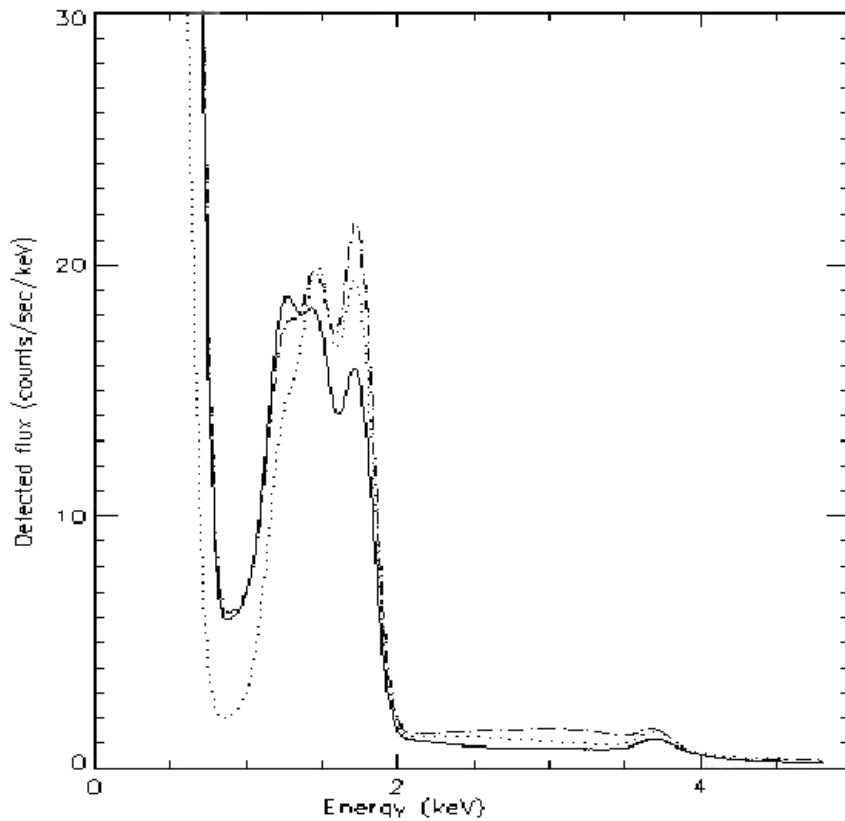
b)

**Figure 10** Four different solar flare input levels (a5, b1,c1, m1), with the calculated lunar fluorescent spectra, as detected by C1XS, which would result.

Figure 11



a)



b)

**Figure 11** Three different models of C1 solar flares (Mewe et al 1985, Clark et al 1997,) with the calculated lunar fluorescent spectra, as detected by C1XS, that would result. Note complete reversal of the line ratios which would be observed.



Element	$K\alpha_1$	$L\alpha_1$
Oxygen	524.9	-
Sodium	1,040.98	-
Magnesium	1,253.60	-
Aluminium	1,486.70	-
Silicon	1,739.98	-
Potassium	3,313.8	-
Calcium	3,691.68	-
Titanium	4,510.84	-
Iron	6,403.84	705.0

**Table 1** Energies (KeV) of relevant X-ray fluorescent lines. See discussion for those lines detectable by C1XS.

# 1 THE C1XS X-RAY SPECTROMETER ON CHANDRAYAAN-1.

2

3 M. Grande<sup>1</sup>, B. J. Maddison<sup>2</sup>, C.J. Howe<sup>2</sup>, B. J. Kellett<sup>2</sup>, P. Sreekumar<sup>3</sup>, J. Huovelin<sup>4</sup>, I. A. Craw-  
4 ford<sup>5</sup>, C L Duston<sup>6</sup>, D Smith<sup>7</sup>, M. Anand<sup>8</sup>, N. Bhandari<sup>10</sup>, A. Cook<sup>1</sup>, V. Fernandes<sup>12</sup>, .B Foing<sup>15</sup>,  
5 O Gasnaut<sup>6</sup>, JN Goswami<sup>10</sup>, A Holland<sup>8</sup>, K. H. Joy<sup>2,5,9</sup>, D Kochney<sup>15</sup>, D Lawrence<sup>11</sup>, S Maurice<sup>6</sup>,  
6 T. Okada<sup>14</sup>, S Narendranath<sup>3</sup>, C Pieters<sup>16</sup>, D Rothery<sup>8</sup>, S. S. Russell<sup>9</sup>, A Shrivastava<sup>3</sup>, M Wiec-  
7 zorek<sup>13</sup>, B. Swinyard<sup>2</sup>, M. Wilding<sup>1</sup>

8 <sup>1</sup>Institute of Mathematical and Physical Sciences, University of Wales, Aberystwyth, SY23 3BZ,  
9 UK, M.Grande@aber.ac.uk, <sup>2</sup>Rutherford Appleton Laboratory, Chilton, UK, <sup>3</sup>Space Astronomy  
10 & Instrumentation Division, ISRO Satellite Centre, Bangalore, India, <sup>4</sup>The Observatory, Univ. of  
11 Helsinki, Finland, <sup>5</sup>The Joint UCL/Birkbeck Research School of Earth Sciences, Gower Street,  
12 London, WC1E 6BT UK, <sup>6</sup>Centre d'Etude Spatiale des Rayonnements, Université de Toulouse,  
13 CNRS, France,, <sup>7</sup>Brunel Univ, UK, <sup>8</sup>Open University UK, <sup>9</sup> Department of Mineralogy, Natural  
14 History Museum, Cromwell Road, London SW7 5BD, UK. UK. <sup>10</sup>PRL India, <sup>11</sup>Los Alamos Na-  
15 tional Lab, USA, <sup>12</sup>Berkeley Geochronology Center, Berkeley, CA, USA, <sup>13</sup>IPG Paris,  
16 France. <sup>14</sup>ISAS/JAXA, Japan, <sup>15</sup> ESTEC, ESA, Holland <sup>16</sup> Brown University USA.

17

## 18 **Abstract:**

19 The Chandrayaan-1 X-ray Spectrometer (C1XS) is a compact X-ray spectrometer  
20 for the Indian Space Research Organisation (ISRO) Chandrayaan-1 lunar mission. It exploits  
21 heritage from the D-CIXS instrument on ESA's SMART-1 mission. As a result of detailed de-  
22 velopments to all aspects of the design, its performance as measured in the laboratory greatly  
23 surpasses that of D-CIXS. In comparison with SMART-1, Chandrayaan-1 is a science oriented



24 rather than a technology mission, leading to far more favourable conditions for science measure-  
25 ments. C1XS is designed to measure absolute and relative abundances of major rock-forming  
26 elements (principally Mg, Al, Si, Ca and Fe) in the lunar crust with spatial resolution  $\leq 25$   
27 FWHM km, and to achieve relative elemental abundances of better than 10%.

28

## 29 **Introduction:**

30

31 The Chandrayaan-1 X-ray Spectrometer (C1XS) is a compact X-ray spectrometer  
32 for the Indian Space Research Organisation (ISRO) Chandrayaan-1 lunar mission, which was  
33 successfully launched on 22 October 2008. It exploits heritage from the D-CIXS instrument  
34 (Grande et al., 2001, 2003, 2007; Swinyard et al., *forthcoming*) on ESA's SMART-1 mission  
35 (Racca et al 2002). However, by comparison with SMART-1, Chandrayaan-1 is a science ori-  
36 ented rather than a technology mission, leading to far more favourable conditions for science  
37 measurements. C1XS is designed to measure absolute and relative abundances of major rock-  
38 forming elements (principally Mg, Al, Si, Ca, Ti and Fe) in the lunar crust with spatial resolution  
39 ~25 km.

40 The C1XS hardware was designed and built by an international team led from the  
41 Rutherford Appleton Laboratory (RAL), STFC. The Principal Investigator is Prof. M. Grande at  
42 Aberystwyth University. There is also a major science and design contribution from ISRO Satel-  
43 lite Centre, Bangalore, India; CESR, Toulouse, France provides 3-D Plus video processor inte-  
44 grated circuits, and there is an important contribution to the detector characterisation from Brunel  
45 University. The Science team is chaired by Dr. I. A. Crawford of Birkbeck College London. In  
46 order to record the incident solar X-ray flux at the Moon, C1XS carries an X-ray Solar Monitor

47 (XSM) provided by the University of Helsinki Observatory, Finland. C1XS is primarily funded  
48 by ESA with partial support to RAL from ISRO.

49 D-CIXS was able to demonstrate an ability to sense remotely elements in the top  
50 few micrometers of the lunar regolith, in particular Mg, Al, Si, Ca and Fe (Grande et al., 2007;  
51 Swinyard et al., *forthcoming*). The Ca detections represented the first unambiguous remote sens-  
52 ing of calcium. More recent detailed analysis shows that in favorable conditions titanium is also  
53 observed (Swinyard et al. *forthcoming*). Other companion papers describe in more detail the sci-  
54 ence goals (Crawford et al., *forthcoming*) the instrument construction (Howe et al., *forthcoming*)  
55 and the calibration status (Kellett et al., *forthcoming*).

56

## 57 **Instrument requirements**

58

59 Solar irradiation excites fluorescent emission from the lunar surface; by measuring  
60 this emission, whilst at the same time monitoring the incident solar X-ray emission, we are able  
61 to map the absolute elemental abundances of the main rock forming elements on the Moon. In  
62 addition, during bright flares, we detect localised concentration levels of key minor elements.  
63 The timing of the Chandrayaan-1 mission, ensuring that the spacecraft arrives at the beginning of  
64 the rising phase of the solar activity cycle, with near Solar maximum flux levels expected at the  
65 end of its nominal mission, is well suited for this purpose. The 10× higher solar X-ray fluxes,  
66 combined with the excellent (85 – 115 km near circular) orbit, will help ensure that C1XS can  
67 carry out enormously enhanced science compared to SMART-1.

68 The nominal mission duration is 2 years. Given the Moon's 28 day rotation, this  
69 corresponds to 25 daylight overflights for each 25 km FWHM Field of View on the surface, and

70 16 within  $60^\circ$  of zenith illumination. Illumination conditions will be different for each overflight,  
71 both for geometrical reasons, but much more importantly because of the huge variations in the  
72 solar X-ray illumination that take place on timescale of minutes, as shown in Figure 1b. At solar  
73 maximum, expected at or shortly after the end of the Chandrayaan-1 mission, X-ray illumination  
74 is above C1 category flare conditions for ~40% of the time (see figure 2), based upon statistics  
75 from the previous cycle.. In a 2 year solar maximum mission, each pixel would be sampled with  
76 near zenith C1 illumination on average 6 times. A more precise calculation shows around 95%  
77 probability of a pixel being illuminated at greater than C1 at some point during the mission,  
78 which is sufficient to return the required spectral resolution. Around 10% of pixels should be il-  
79 luminated with greater than M1 at some point during the mission. We note that C1XS is to be  
80 launched at around the beginning of solar cycle, and that fluxes are therefore very sensitive to  
81 variations of a few months in the upturn in the solar cycle relative to the launch date. Figure 2 is  
82 based on the current (27 Jun 2008) best NOAA SEC predictions (Biesecker 2008) showing the  
83 high and low predictions. Currently (Keating, 2008) the cycle appears to be an average 11 year  
84 cycle. A 6 month mission extension, at full Solar maximum, would certainly yield large increases  
85 in the quality of x-ray illumination.

86 We can investigate minor elements like sodium, phosphorous and sulphur which  
87 provide great insight into lunar evolution. The energy range of C1XS is 0.8 to 7 keV, and the en-  
88 ergy resolution at launch is ~160 eV FWHM at 8 KeV (2%), sufficient to resolve all the main  
89 fluorescence lines of interest, as shown in table 1. The ability to detect sodium ( $K\alpha$  at 1.043  
90 keV) if it is present in significant quantities is particularly interesting. It may also be possible to  
91 detect the iron L-lines, which will enable C1XS to observe iron in all illumination conditions.  
92 For these reasons, particular care has been taken in defining the lower energy cut-off, as illus-

93 treated in figure 3a. The low energy discriminator level is software commandable, but whilst in  
94 theory it could be lowered to include the oxygen  $K\alpha$  line at 525 keV, and the detectors have some  
95 sensitivity at these low energies, the filter cutoff shown in figure 3b would preclude useful in-  
96 formation. Since the oxygen concentration across the highly oxidised lunar surface does not vary  
97 outside a range 41% - 46% (eg Lawrence et al), this data would not in any case yield significant  
98 new information. However, at start of mission, we will have sufficient sensitivity for the Fe  $L\alpha$   
99 line at 705 eV which greatly improves the functionality of the instrument, enabling Fe concentra-  
100 tions to be measured in all illumination conditions. Figure 3c shows the calculated overall effec-  
101 tive area of the instrument, excluding electronic considerations.

102 In order to obtain good absolute elemental abundances by the X-ray fluorescence  
103 technique, it is essential to continuously monitor the solar X-ray flux which excites the lunar  
104 emission. To this end the CIXS instrument includes an X-ray Solar Monitor (XSM), designed  
105 and delivered by the University of Finland. The XSM will also provide a scientific bonus in pro-  
106 viding a long time series of the solar X-ray spectra with high spectral resolution and full energy  
107 band coverage.

108

## 109 **Instrument**

110 The baseline instrument design (see figure 4) consists of 24 nadir pointing Swept  
111 Charge Device (SCD) detectors (Howe et al., *forthcoming*). A traditional box collimator defines  
112 the field of view of each SCD, resulting in a triangular angular sensitivity with 50% of the X-ray  
113 signal deriving from  $14^\circ$  of the collimator aperture, corresponding to 25 km on the lunar surface  
114 from Chandrayaan-1's circular 100 km orbit. Due to the highly elliptical orbit of SMART-1 the  
115 corresponding values for D-CIXS ranged from 32 to 315 km. The uniform spatial resolution of

116 C1XS will greatly simplify the data analysis. The C1XS collimator stack differs from that on D-  
117 CIXS in that it is machined numerically, as opposed to by lithographic construction (Grande et al  
118 2003, Howe et al forthcoming). Figure 5 shows the flight instrument during calibration.

119           A deployable door protects the instrument during launch and cruise, and also pro-  
120 vides a  $^{55}\text{Fe}$  calibration X-ray source for each of the detectors, allowing in flight calibration to be  
121 performed. The source strength is sufficient over the two year mission for gain calibration to the  
122 required 1% accuracy to be obtained within 10 minutes. This will also allow energy and FWHM  
123 calibrations of sufficient accuracy to be obtained.

124

## 125 **Detectors**

126           The Swept Charge Device (SCD) detectors (Gow et al 2007) provide high detec-  
127 tion efficiency in the 0.8 to 7 keV range, which contains the X-ray fluorescence lines of interest.  
128 The SCD is a CCD-like device which achieves near Fano-limited spectroscopy below  $-10^{\circ}\text{C}$ . It  
129 has a continuous one dimensional readout architecture which is otherwise similar to a conven-  
130 tional CCD, and a  $1.1\text{cm}^2$  detector area. The instrument design aims to keep detector tempera-  
131 tures below  $-17.5^{\circ}\text{C}$ , which provides sufficiently low SCD leakage current to ensure optimum  
132 signal to noise and stability, as well as improving radiation tolerance.

133           The detectors are shielded from the lunar UV and visible albedo, as well as pro-  
134 tons below 180keV and low energy electrons, by two layers of 400nm aluminized polyimide fil-  
135 tering (figure 3b shows their calculated x-ray transmission). Careful thought has been given to  
136 the radiation shielding, in what is already a comparatively low radiation environment orbit. It will  
137 now consist of a 4 mm thick aluminum electronics box with 3mm of copper and 6 mm of tanta-  
138 lum behind the SCD modules. Due to the low altitude, the spacecraft is well shielded from the

139 front by the Moon itself. The collimator structure and additional tantalum provides additional  
140 shielding for oblique angles.

141 The principal instrument requirement is a spectral resolution sufficient to clearly  
142 resolve the three common light rock forming elements (Mg, Al, Si) As will be seen from table 1  
143 below, this implies an energy resolution better than 250 eV at 1-2 keV. Figures 6a and 6b indi-  
144 cates that in laboratory calibration this condition is comfortably met. The effects of radiation tests  
145 on SCD detectors from the same batch are shown in Figure 7 suggesting that even at end of life,  
146 the performance requirements will be met. There is some uncertainty in the predicted range of  
147 exposures due to the sensitivity to the phase of the solar cycle. The figures shown reflect the fact  
148 that as of the present, large solar flares have not been observed in the current rising cycle. Note  
149 by comparison the reduced energy resolution of D-CIXS after the heavy radiation doses it in-  
150 curred during its extended cruise phase to the Moon (Grande et al., 2007).

151 The maximum expected count rate for the C1XS instrument will be 2000 counts  
152 per second for all 24 detectors, for an X20 flare, acceptably within the instrument limit of 5500  
153 cps (see Howe et al., *forthcoming*). Additional refinements to the electronics, onboard software  
154 and thermal design will also greatly increase detector stability and signal to noise ratio over what  
155 was achieved on D-CIXS [Grande et al., 2007]. Electronic noise has been reduced to 60eV. A  
156 detailed account of the technical development is given in Howe et al.,(*forthcoming*).

157

## 158 **X-ray Solar Monitor**

159 The X-ray solar monitor (XSM) is based on the SMART-1 XSM (Huovelin et al  
160 2002) and consists of a separate silicon detector unit on the spacecraft. The non-imaging HPSi  
161 PIN sensor has a wide field-of-view (FOV) to enable Sun visibility during a significant fraction

162 of the mission lifetime, which is essential for obtaining calibration spectra for the X-ray fluores-  
163 cence measurements by the C1XS spectrometer. The energy range (1–20 keV), spectral resolu-  
164 tion (about 200 eV at 6 keV), and sensitivity (about 7000 cps at flux level of  $10^{-4}$  W m<sup>-2</sup> in the  
165 range 1–8 keV) are tuned to provide optimal knowledge about the solar X-ray flux, matching  
166 well with the activating energy range for the fluorescence measured by C1XS.

167 As has been remarked, the X-ray flux rises rapidly during a major solar flare.  
168 However, this is frequently followed by an increase in penetrating background radiation, at a  
169 time delay dependent on the energy and the geometry of the interplanetary magnetic flux. Thus it  
170 is still in general possible to use the brightest X-class events for fluorescence spectroscopy, and  
171 the very high fluorescence count rates obtained will be invaluable in revealing the concentrations  
172 of minor elements in the regolith. Typical time delays are of up to one hour duration.

173

#### 174 **Predicted Response:**

175 The baseline specification is to achieve 10% relative elemental abundance accu-  
176 racy from a single overflight of a 25 km pixel in C1 solar flare conditions, and we consider the  
177 instrument response in terms of this baseline situation. Figure 8 shows the calculated response to  
178 fluorescence from a representative Lunar basalt, using our physical instrument model, indicating  
179 the minimum detectable flux for C1 flare with a 14 deg opening angle for a real detector area of  
180 24 cm<sup>2</sup> detector and a 0.8 throughput collimator expressed as counts/sec/keV and a 100 eV reso-  
181 lution. The calculation includes calibration and electronic efficiency data from D-CIXS. The  
182 smooth line is the 3 sigma detection limit for a 16 second integration, typical for overflight of a  
183 single pixel. It is seen that the Mg, Al and Si lines are well resolved for this baseline illumination  
184 condition. As an example of inferred performance under flare conditions, Figure 9 shows a com-

185 parison of predicted C1XS response in quiet and flare conditions to an actual event observed by  
186 D-CIXS, described in the accompanying paper by Swinyard et al., (*forthcoming*). Note the  
187 greatly increased signal for the low-energy Mg, Al and Si lines, and the excellent signal-to-noise  
188 ratio in the Ca, Ti and Fe lines at the peak of the flare. Again, instrument response (100 eV) is  
189 derived from C1XS laboratory calibrations (Kellett et al., *forthcoming*).

190           Accurate knowledge of the input solar spectrum is essential for determination of  
191 elemental abundances. A linear difference in solar input will leave the relative line ratios un-  
192 changed. However, this is not the case if the shape of the input solar spectrum changes. Figure 10  
193 shows 4 different flare levels (a5, b1, c1, m1), with the output spectra that would result. We note  
194 that the apparent line ratios are very significantly modified. The point is made even more clearly  
195 in Figure 11 which shows three different models of C1 solar flares (Mewe et al., 1985, Clark et  
196 al., 1997,). The calculated lunar fluorescent spectra, which would be detected following scintilla-  
197 tion of lunar basalt, are also shown. In this case the predicted line ratios are modified by more  
198 than +/- 10%.

199           This emphasizes the vital importance of accurate monitoring of the solar input  
200 spectrum, as well as good codes to forward model the expected lunar X-ray fluorescence for dif-  
201 ferent possible regolith compositions. Thus, whilst elemental abundance ratios may be useful di-  
202 agnostics in our initial analysis, final estimations of lunar elemental abundance ratios will require  
203 detailed modelling (see Swinyard et al., *forthcoming*). One of the lessons learned from D-CIXS  
204 was the critical importance of fully characterizing the input solar spectrum, if one is to derive ab-  
205 solute lunar elemental surface abundances. In comparison to D-CIXS, C1XS and XSM are far  
206 better calibrated. Details of the results obtained in the calibration campaign of the C1XS instru-  
207 ment are given by Kellett et al. (*forthcoming*).



208

209 **Science Goals:**

210 A detailed description of the science objectives for the instrument and the match  
211 of its capabilities to key questions is given in a companion paper by Crawford et al., (*in press*).  
212 C1XS will arrive at the Moon in the run up to the maximum of the solar cycle, and the high inci-  
213 dent X-ray flux observed from an orbit optimized for science, and coupled with good instrumen-  
214 tal energy resolution, means that we will obtain composition data accurate to better than 10% of  
215 major elemental abundances over the entire surface. We note that observations of major element  
216 abundances for regions where samples have been obtained by the Apollo and Luna missions will  
217 be used to validate the calibration of C1XS measurements. Thus, C1XS will be well-placed to  
218 make significant contributions to lunar science in a number of areas.

219 Specifically, C1XS will determine the major element geochemistry (and especially  
220 Mg/Si and/or Mg/Fe elemental ratios) in the main lunar terrain types (i.e. Procellarum KREEP  
221 Terrane, South Pole-Aitken Basin, and the Farside Highlands; Jolliff et al., 2000) and establish  
222 the geographical distribution of the magnesian suite of rocks. A key ambition is to determine the  
223 large-scale stratigraphy of lower crust (and possibly crust/mantle boundary region) by measuring  
224 the elemental abundances of the floor material of large basins not obscured by mare basalts (e.g.  
225 SPA and other farside basins), and the central rings and ejecta of large basins which expose ma-  
226 terial derived from depths of many tens of km. In addition, determination of the crustal alumin-  
227 ium abundance and distribution is important for the assessment of lunar refractory element en-  
228 richment, and C1XS-derived aluminium abundance maps will thus constrain models of lunar ori-  
229 gins. Last but not least, the ~25 km spatial resolution will enable C1XS to address a number of  
230 smaller-scale geological issues (e.g., the composition of discrete mare basalt lava flows and, py-

231 roclastic deposits) which also refine our understanding of lunar geological evolution (Joy et al.,  
232 2008, Crawford et al., *in press*).

233

## 234 **Conclusions**

235

236           The C1XS instrument is optimised to perform X-ray spectroscopy in the frame-  
237 work provided by the ISRO Chandrayaan-1 mission to the Moon. This is highly suitable for pro-  
238 ducing high quality data on lunar composition derived from Lunar X-ray fluorescence spectra,  
239 taken in the approach to Solar maximum. The instrument represents a considerable refinement on  
240 the original D-CIXS instrument on SMART-1. It is expected to provide data of the spatial and  
241 spectral resolution required to produce significant progress in lunar science.

242 **Acknowledgements**

243

244 The C1XS instrument development was supported with funding from ESA Science and Technol-  
245 ogy Research Programmes. Major thanks for support are due to RAL/STFC, and also ISRO  
246 ISAC. Additional hardware was provided by CESR, Toulouse, and University of Helsinki Ob-  
247 servatory. J Carter of Aberystwyth University for recalculating figure 8.

248

249 **References:**

250 Biesecker D, and the NOAA/SEC Solar Cycle 24 Panel . The Solar Cycle 24 Consensus Predic-  
251 tion; Web document [www.swpc.noaa.gov/SolarCycle/SC24/Biesecker.ppt](http://www.swpc.noaa.gov/SolarCycle/SC24/Biesecker.ppt) *June 2008*

252

253 Clark P E and J.I. Trombka *J. Geophys. Res.* **102**, 16631 (1997)

254

255 Crawford I A , K.H. Joy, B.J. Kellett, M. Grande, M. Anand, N. Bhandari, A.C. Cook, L.  
256 d’Uston, V.A. Fernandes, O. Gasnault, J. Goswami, C.J. Howe, J. Huovelin, D. Koschny, D.J.  
257 Lawrence, B.J. Maddison, S. Maurice, S. Narendranath, C. Pieters, T. Okada, D.A. Rothery, S.S.  
258 Russell, P. Sreekumar, B. Swinyard, M. Wieczorek, M. Wilding: The Scientific Rationale for the  
259 C1XS X-Ray Spectrometer on India’s Chandrayaan-1 Mission to the Moon, *Planet. Space. Sci.*,  
260 (submitted PSS 2008 This volume 2008).

261

262 Gow, J; Smith, DR; Holland, AD; Maddison, B; Howe, C; Sreekumar, P; Huovelin, J; Grande,  
263 M, Characterisation of swept-charge devices for the Chandrayaan-1 X-ray Spectrometer (C1XS)

264 instrument - art. no. 66860I, OHW, UV, X-RAY, AND GAMMA-RAY SPACE  
265 INSTRUMENTATION FOR ASTRONOMY XV 6686I6860-I6860 2007  
266  
267 Grande M The D-CIXS X-ray Spectrometer on ESA's SMART-1 mission to the Moon EARTH  
268 MOON AND PLANETS 2001, Vol 85-6, pp 143-152  
269  
270 Grande M., et al, The D-CIXS X-ray mapping spectrometer on SMART-1, Planetary and Space  
271 Science, 2003, 51, 427-433,  
272  
273 Grande M., et al. The D-CIXS X-ray spectrometer on the SMART-1 mission to the Moon—First  
274 Results. Planetary and Space Science **55**, 494 (2007)  
275  
276 Howe et al (submitted PSS 2008 This volume 2008).  
277 Huovelin J; Alha L; Andersson H; Andersson T; Browning R; Drummond D; Foing B; Grande  
278 M; Hamalainen K; Laukkanen J; Lamsa V; Muinonen K; Murray M; Nenonen S; Salminen A;  
279 Sipila H; Taylor I; Vilhu O; Waltham N; Lopez-Jorkama M The SMART-1 X-ray solar monitor  
280 (XSM): calibrations for D-CIXS and independent coronal science. PLANETARY AND SPACE  
281 SCIENCE 2002, Vol 50, Iss 14-15, pp 1345-1353  
282  
283 Jolliff, B.L., Gillis, J.J., Haskin, L.A., Korotev, R.L., Wiczorek, M.A. 2000. Major lunar crustal  
284 terranes: surface expressions and crust-mantle origins. *J. Geophys. Res.* **105**, 4197  
285

286 **Joy K. H.**, Crawford I.A., Kellett B., Grande M.N. and the C1XS Science Team. (2008). The  
287 Scientific Case for the Chandrayaan-1 X-Ray Spectrometer. In *Lunar and Planetary Science*  
288 xxxvix, abstract no. 1070, 39th Lunar and Planetary Science Conference, Houston.

289

290 Keating 2008 EOS in press

291

292 Kellett et al (submitted PSS 2008 This volume 2008).

293

294 Lawrence D. J., W. C. Feldman, B. L. Barraclough, A. B. Binder,

295 R. C. Elphic, S. Maurice, D. R. Thomsen , Global Elemental Maps of the

296 Moon: The Lunar Prospector Gamma-Ray Spectrometer 4 SEPTEMBER 1998 VOL 281

297 SCIENCE 1998

298

299 R. Mewe, E. H. B. M. Gronenschild, G. H. J. van den Oord, *V. Astron. Astrophys. Supp.* **62**, 197.

300 (1985)

301

302 Racca GD, Marini A, Stagnaro L, van Dooren J, di Napoli L, Foing BH, Lumb R, Volp J,

303 Brinkmann J, Grunagel R, Estublier D, Tremolizzo E, McKay M, Camino O, Schoemaekers J,

304 Hechler M, Khan M, Rathsmann P, Andersson G, Anflo K, Berge S, Bodin P, Edfors A, Hussain

305 A, Kugelberg J, Larsson N, Ljung B, Meijer L, Mortsell A, Nordeback T, Persson S, Sjoberg F.

306 SMART-1 mission description and development status. PLANETARY AND SPACE

307 SCIENCE Volume: 50 Issue: 14-15 Pages: 1323-1337 Published: DEC 2002

308

309 Swinyard et al (submitted PSS 2008 This volume 2008).

310